Free vibration analysis of gravity dam-reservoir system utilizing 21 node-33 Gauss point triangular elements

Seyed Hamid Ziaolhagh[*1], Meghdad Goudarzi[2] and Ahmad Aftabi Sani[2]

[1]Civil Engineering Department, Shahrood University of technology, Shahrood, Iran
[2]Civil Engineering Department, Mashhad Branch, Islamic Azad University, Mashhad, Iran

Abstract.   This paper deals with the free vibration analysis of a dynamical coupled system: flexible gravity dam- compressible rectangular reservoir. The finite element method is used to compute the natural frequencies and modal shapes of the system. Firstly, the reservoir and subsequently the dam is modeled by classical 8-node elements and the natural frequencies plus modal shapes are calculated. Afterwards, a new 21-node element is introduced and the same procedure is conducted in which an efficient method is employed to carry out the integration operations. Finally, the coupled dam-reservoir system is modeled by solely one 21-node element and the free vibration of dam-reservoir interaction system is investigated. As an important result, it is clearly concluded that the one high-order element treats more precisely than the eight-node elements, since the first one utilizes fifth-degree polynomials to construct the shape functions and the second implements polynomials of degree two.

Keywords: dam–reservoir interaction; Finite element method; mathematica; Gauss integration

1. Introduction

Dams can be counted as very important man-made structures which are constructed by paying high prices and have exerted a powerful influence over the lives of thousands. Modeling such significant structures should be in a way that reflects the actual behavior of the correlated fluid-structure system, considering the fact that fluid and the structure are in direct contact with each other and the overall response of the system is dependent on their interaction. Thereby, these structures could be designed in such a way to withstand strong earthquakes with minimal damages.

One of the major factors in the analysis and design of concrete gravity and arch dams in seismic areas is the effect of hydrodynamic pressure due to ground movement during an earthquake. Analysis of interacting fluid-structure systems under dynamic loads is the case that has attracted the interest of many researchers during years. Due to the complexity of such systems, utilizing accurate and non-numerical analysis is almost impossible and applying numerical and approximate techniques will be inevitable. For instance, Hall and Chopra (1982) treated dam and fluid domain as substructures and modelled them with finite elements to investigate the hydrodynamic effects in the acceleration response of concrete gravity dams. Moreover, Fenves and

---

Chopra (1984) extended the previous studies to include the effects of alluvium and sediments invariably present at the bottom of actual reservoirs Fenves and Chopra (1984). Leger and Bhattacharjee (1992) presented a rational methodology to develop simple dam-foundation-reservoir models for nonlinear analysis. Valliappan and Zhao (1992) investigated dynamic response of concrete gravity dams including dam-water-foundation interaction by using a finite element and infinite element coupling model Valliappan and Zhao (1992). Subsequently, Zhao *et al*. (1995) carried out an investigation into the effect of reservoir bottom sediment on the seismic response of concrete gravity dams using the finite and infinite element coupled method. Furthermore, Ghaemian and Ghobarah (1999) conducted a nonlinear seismic fracture response analysis of concrete gravity dams which includes the dam–reservoir interaction, to investigate the performance of different reservoir interaction models. Also, Yazdchi *et al*. (1999) presented a computational method for the non-linear seismic response of concrete gravity dams using continuum damage mechanics. Similarly, Calayir and Karaton (2005) investigated the earthquake damage response of the concrete gravity dams with considering the effects of dam-reservoir interaction by selecting a continuum damage model which was a second-order tensor and included the strain softening behavior for the concrete material. Samii and Lotfi (2007) compared two methods for modal analysis of concrete gravity dams, one based on using coupled modes, while the other utilized decoupled modes of dam and reservoir. Bouaanani and Lu (2009) assessed the use of a potential-based fluid finite element formulation for seismic analysis of dam–reservoir systems. Afterward, Miquel and Bouaanani (2010) proposed a procedure for a simplified evaluation of the fundamental vibration period of dam-water systems, which is compared with potential-based finite elements approach. Continuing their pervious study, Miquel and Bouaanani (2011) developed analytical and simplified solutions for dynamic analysis of structures vibrating in contact with water. Moreover, Mirzayee *et al.* (2011) analyzed seismic behavior of fractured concrete gravity dams considering dam–reservoir interaction effects, they obtained dynamic response of the reservoir using boundary element method. Attarnejad and Kalateh (2012) presented a numerical model and its finite element implementation that used to compute the cavitation effects on seismic behavior of concrete dam and reservoir systems. Furthermore, Karaca and Küçükarslan (2012) analyzed dam-reservoir interaction for a vibrating structure in an unbounded and incompressible and inviscid fluid by using homotopy analysis method. Burman *et al*. (2012) analyzed Coupled gravity dam–foundation using a simplified direct method of soil-structure interaction. In addition, Hariri *et al*. (2013) solved the coupled dam-reservoir-foundation system in Lagrangian-Eulerian domain using Newmark-β time integration method. Mridha and Maity (2014) investigated the nonlinear response of concrete gravity dam-reservoir system by conducting experiments and compared the experimental results with numerical analysis. Moreover, Keivani *et al.* (2014) obtained the closed-form solution of fluid-structure interaction problem in the frequency domain and compared it with finite element analysis.

   In this paper, modeling of the problem domain including ideal triangular gravity dam and rectangular reservoir is performed by finite elements method. For this purpose, firstly, the classical 8-node elements are used. The integrations of the structure mass and stiffness matrices plus the fluid quasi-mass and quasi-stiffness matrices are accomplished by both exact and application of the Gauss integration methods. In the next stage, after introducing a high-ordered 21-node triangular element, in which shape functions are obtained based on complete polynomial of degree 5, the dynamic analysis of gravity dam, rectangular reservoir and dam-reservoir system is accomplished. It is noteworthy that the advantages of this kind of elements due to utilizing high-degree complete polynomials in the form of shape functions include better approximation of

unknown quantity variations, creating higher order continuity at nodes and boundaries, possibility of modeling curved boundaries-particularly for complex geometries, increasing the accuracy of solutions and more rapid convergence. It should be pointed out that using high-degree interpolation functions cause complexity in integration associated with finite element matrices and protracts calculations. In this study, at first, integrals are calculated by this accurate but extremely time consuming procedure, but then, Gauss numerical integration in triangular elements with a large number of points will be used. By doing this, without causing any harm to the accuracy of the answers, the time for finding them will be reduced significantly.

The paper is organized as follows. Initially, the required theoretical foundations will be presented. Afterward, exact and numerical solution of the rectangular reservoir free vibration is given. Subsequently, the ideal triangular dam will be analyzed with the aid of 8 and 21-node elements. Thereafter, the main innovative aspect of this paper is introduced in the fifth section, in which the interaction of dam-reservoir system will be analyzed with the aid of 21-node element utilizing 33 Gauss points. Finally, last section is devoted to the qualitative results of the study.

2. Theoretical foundations

This section is dedicated to an overview of the requirements of the finite element method, including the Gauss points of the triangle, the dynamic analysis of structures and fluids using finite element, Stokes-Navier equation, Helmholtz equation in matrix form, and interaction analysis of dam-reservoir system by finite element method (Rao 2011).

2.1 Finite element in structure dynamic analysis

The dynamic analysis of structures, in the most general three-dimensional case, is reviewed here briefly. In dynamic problems, the displacements, velocities, strains, stresses, and loads are all time dependent. The procedure involved in deriving the finite element equations of a dynamic problem can be stated by these steps: idealizing the body into e finite elements; assuming the displacement model of element e as

$$\{U(x,y,z,t)\} = [N(x,y,z)]\{D^e(t)\} \tag{1}$$

and finally, deriving the element characteristic (stiffness and mass) matrices and characteristic (load) vector. For this purpose, the strain at any point inside the element can be expressed as

$$\{\varepsilon\} = [B]\{D^e\} \tag{2}$$

where $\{\varepsilon\}$ is strain vector, and $[B]$ is strain-displacement matrix which relates strain components inside the element to element nodal displacements. Moreover, the stress–strain relations in matrix form is

$$\{\sigma\} = [D]\{\varepsilon\} \tag{3}$$

where $[D]$ is the material or constitutive matrix. In the case of two-dimensional problems, the material matrix would have only three rows and three columns. For example in plane strain

problems matrix $[D]$ reduces to

$$[D] = \frac{E}{(1+v)(1-2v)} \begin{bmatrix} 1-v & v & 0 \\ v & 1-v & 0 \\ 0 & 0 & \dfrac{1-2v}{2} \end{bmatrix}$$

(4)

In the following, the governing equation of each component would be derived by utilizing Hamilton's principle and Lagrangian function

$$L = T - \pi_p$$

(5)

the kinetic and potential energies (T and π_p) can be expressed as

$$T = \frac{1}{2}\{\dot{D}\}^T [\sum_{e=1} \iiint_V \rho [N]^T [N] dV]\{\dot{D}\}$$

(6)

and

$$\pi_p = \frac{1}{2}\{D\}\left[\sum_{e=1} \iiint_v [B]^T [D][B] dV\right]\{D\} - \{D\}^T \left[\sum_{e=1} \iint_{S_1} [N]^T \{t\} dS_1 + \iiint_V [N]^T \{b\} dV\right]$$

(7)

where V is the volume, ρ is the density of material, S_1 is the surface of the body on which surface forces $\{t\}$ are prescribed and $\{b\}$ is the body force vector.

The matrices involving the integrals can be defined as follows:
element mass matrix

$$[M^e] = \iiint_V \rho [N]^T [N] dV$$

(8)

element stiffness matrix

$$[K^e] = \iiint_V [B]^T [D][B] dV$$

(9)

vector of element nodal forces produced by surface forces

$$[P_s] = \iint_{S_1} [N]^T \{t\} dS_1$$

(10)

vector of element nodal forces produced by body forces

$$[P_b] = \iiint_V [N]^T \{t\}$$

(11)

Thus, total load vector of the structure is

$$\{P(t)\} = \sum_e [\{P_s + P_b\}]$$

(12)

Now, by utilizing the above relations, the desired dynamic equation of motion of the undamped structure is

$$[M]\{\ddot{D}\}(t) + [K]\{D(t)\} = \{P(t)\}$$
(13)

It should be noted that, in the case of free vibration with no external forces, the recent relation gives the following eigenvalue problem

$$([K] - \omega^2[M])\{\cancel{\emptyset}\} = \{0\}$$
(14)

By solving Eq. (14), the natural frequencies and mode shapes could be found.

2.2 Finite element in fluid dynamic analysis

Significant contributions are made in the solution of different types of fluid flow problems using the finite element method. This section presents a summary of the basic concepts and some equations of fluid mechanics including Navier-Stokes equation (Rao 2011).

2.2.1 Acoustic wave equation

The equation governing fluids in motion, is a partial differential equation which is called Navier-Stokes equation. This equation could be derived by employing Reynolds transport theorem, principles of mass conservation, continuity equation, and principle of conservation of momentum, Newton's second law and Newtonian fluid relations as

$$\left[\vec{b} - \vec{\nabla}p + \frac{1}{3}\mu\vec{\nabla}\dot{e} + \mu\nabla^2\vec{V}\right] = \rho\left[\frac{\partial\vec{V}}{\partial t} + \frac{1}{2}\vec{\nabla}V^2 + (\vec{\nabla}\times\vec{V})\times\vec{V}\right]$$
(15)

where, $\vec{b}, p, \rho, \mu, \dot{e},$ and $\vec{V},$ represent body forces vector acting on the fluid, pressure, density, dynamic viscosity, volumetric dilation rate, and velocity vector, respectively. Furthermore, by assuming that the fluid is inviscid, with small amplitude irrotational motion, Eq. (15) reduces to the Euler equation

$$\vec{b} - \vec{\nabla}p = \rho\frac{\partial\vec{V}}{\partial t}$$
(16)

by applying some mathematical approaches, one could obtain

$$\nabla^2 P = \frac{1}{c^2}\ddot{P}$$
(17)

which is the final equation governing the compressible inviscid fluids and will be utilized in this study.

2.2.2 Helmholtz equation in matrix form

After stating governing equation of the compressible inviscid fluids with small amplitude irrotational motion in the previous section, herein by using Galerkin's weighted residual method, Eq. (17) is expressed in matrix form

$$\underbrace{\iiint_{D^e}([N_x]^T[N_x]+[N_y]^T[N_y]+[N_z]^T[N_z])dVol\{P\}}_{\text{quasi-stifness matrix}}+\underbrace{\frac{1}{c^2}\iiint_{D^e}([N]^T[N]dVol\{\ddot{P}\}}_{\text{quasi-mass matrix}}$$

$$=\underbrace{\iint_{B^e}([N]^T\frac{\partial P}{\partial n})dBou}_{\text{flux vector}}$$

(18)

in which, D^e and B^e are the domain of three-dimensional fluid element and the boundary of the element respectively. Furthermore, N_x represents the partial derivative of interpolation function N with respect to x and $\vec{n}$ is the outward drawn normal to the boundary. The overall and assembled matrix form of Eq. (18) is

$$[G]\{\ddot{P}\}+[H]\{P\}=\{R\}$$

(19)

which is matrix form of Helmholtz equation. Knowing the matrix form of governing equations of fluids and solids, one can couples them and obtain the matrix equation governing the fluid-solid interaction behavior.

2.3 Interaction analysis of dam-reservoir by finite element method

In such a problem, the presence of interaction implies that the response of both subsystems must be evaluated simultaneously. Free vibration analysis of this system gives the dynamic parameters such as frequencies and mode shapes. It is noteworthy that, since the solid-fluid interacting behavior occurs at their common boundary, selected elements should act like a translator to transmit solids' displacement degrees of freedom to fluids' pressure degrees of freedom. Fig. 1 illustrates the boundary conditions of the problem, which includes interaction boundary condition.

By finding the derivatives of velocity potential function directed perpendicular to the direction of common boundary, one can obtain the acceleration and velocity components in that direction

$$\frac{\partial P}{\partial n}=-\rho\frac{\partial V_n}{\partial t}=-\rho a_n$$

(20)

Eq. (20) is the interaction boundary condition. It should be noted that displacements, velocities and accelerations of fluid and structure are equal along the *n* direction.

After obtaining the interaction boundary condition and in order to find fluid-solid interaction relationships, firstly the matrix equation of governing fluid in the vicinity of solid should be simplified (Eq. (19)), knowing that
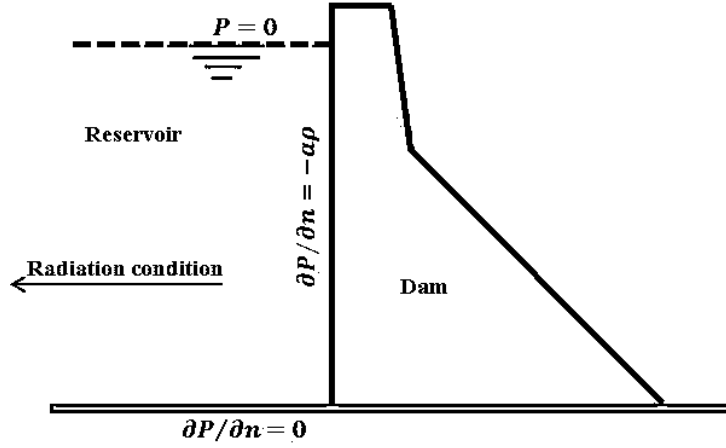
$$\ddot{u}=\{n\}[Q]\{\ddot{D}\}$$

(21)

Fig. 1 Solid-fluid common boundary

in which $[Q]\{\ddot{D}\}$ is acceleration vector of structure's points, and by utilizing Eq. (20), $\{R\}$ vector can be obtained as

$$\{R\} = \iint_{B^e}\left([N]^T \underbrace{\frac{\partial P}{\partial n}}_{-\rho a_n}\right)dBou$$

$$\{R\} = \left(-\rho_f\iint_{B^e}\left([N]^T\{n\}[Q]\right)dBou\right)\{\ddot{D}\}$$

(22)

Moreover, the interaction matrix witch converts solid acceleration to fluid flux is as below

$$[B] = \iint_{B^e}\left([N]^T\{n\}[Q]\right)dBou$$

(23)

Thus, the matrix form of governing equation of compressible inviscid fluid free vibration in vicinity of vibrating solid is

$$[G]\{\ddot{P}\} + [H]\{P\} + \rho_f[B]\{\ddot{D}\} = \{0\}$$

(24)

Furthermore, the governing equation of solid free vibration is

$$[M]\{\ddot{D}\} + [K]\{D\} = \{0\}$$

(25)

it is clear that hydrodynamic forces resulting from vibrating fluid in the vicinity of solid causes the right side of the equation change from zero to $\{F_t\}$.

$$\{F_t\} = \iint_{B^e} \left([Q]^T \begin{Bmatrix} t_x \\ t_y \\ t_z \end{Bmatrix} \right) dBou \tag{26}$$

note that {t} includes traction vector components which leads to

$$\{F_t\} = \iint_{B^e} \left([Q]^T P \begin{Bmatrix} n_x \\ n_y \\ n_z \end{Bmatrix} \right) dBou \tag{27}$$

Meanwhile, hydrodynamic pressure function of fluid can be expressed through interpolating functions as $P = [N]\{P\}$, therefore

$$\{F_t\} = \iint_{B^e} [Q]^T \{n\}^T [N] dBou \{P\} \tag{28}$$

Interestingly, the interaction matrix (Eq. (23)) appears in the relations again, but in transposed form. As can be seen, the transpose of [B] converts fluid pressure to equivalent nodal force of solid. Thus, the governing equation of solid in the vicinity of vibrating fluid would be as

$$[M]\{\ddot{D}\} + [K]\{D\} - [B]\{P\} = \{0\} \tag{29}$$

By combining (24) and (29), one can acquire vibrating solid-fluid interaction equation

$$\underbrace{\begin{bmatrix} [M] & [0] \\ \rho_f[B] & [G] \end{bmatrix}}_{\substack{\text{mass matrix of the} \\ \text{interactional system}}} \underbrace{\begin{Bmatrix} \{\ddot{D}\} \\ \{\ddot{P}\} \end{Bmatrix}}_{\substack{\text{system unknown} \\ \text{vector}}} + \underbrace{\begin{bmatrix} [K] & -[B]^T \\ [0] & [H] \end{bmatrix}}_{\substack{\text{stiffness matrix of} \\ \text{the system}}} \underbrace{\begin{Bmatrix} \{D\} \\ \{P\} \end{Bmatrix}}_{\substack{\text{system unknown} \\ \text{vector}}} = \begin{Bmatrix} \{0\} \\ \{0\} \end{Bmatrix} \tag{30}$$

Thus, for determining the natural frequencies and mode shapes of the system, an eigenvalue problem should be solved

$$Det \left| [K]_{sys} - \omega^2 [M]_{sys} \right| = 0 \tag{31}$$

which would be utilized frequently in this study.

2.4 Gauss points in triangle

One of the main steps in derivation of the matrix equations governing the finite element is the evaluation of integrals that include interpolation functions or their derivatives. Normally, they cannot be found accurately, and therefore, utilizing numerical methods for calculations is essential. There are several schemes available for the numerical evaluation of definite integrals. Among them, Gauss method has been proved to be most useful in finite element applications. The method

needs the function in the integral to be calculated at points called key points (Fig. 2), multiplied to Gauss weights and added. For instance, the following Gauss-type formula has been developed by Hammer and Stroud in which the key points and weights for triangular elements would be in terms of barycentric coordinates

$$\gamma = \iint_A f(L_1, L_2, L_3) \cong \sum_{i=1}^{n} w_i f(L_1^{(i)}, L_2^{(i)}, L_3^{(i)})$$

(32)

where for maximum n = 7

$$w_1 = \frac{27}{60}; \; L_1^{(1)} = L_2^{(1)} = L_3^{(1)} = \frac{1}{3}$$

$$w_2 = \frac{8}{60}; \; L_1^{(2)} = L_2^{(2)} = \frac{1}{2}, L_3^{(2)} = 0$$

$$w_3 = \frac{8}{60}; \; L_1^{(3)} = 0, L_2^{(3)} = L_3^{(3)} = \frac{1}{2}$$

$$w_4 = \frac{8}{60}; \; L_1^{(4)} = L_3^{(4)} = \frac{1}{2}, L_2^{(4)} = 0$$

$$w_5 = \frac{3}{60}; \; L_1^{(5)} = 1, L_2^{(5)} = L_3^{(5)} = 0$$

$$w_6 = \frac{3}{60}; \; L_1^{(6)} = L_3^{(6)} = 0, L_2^{(6)} = 1$$

$$w_7 = \frac{3}{60}; \; L_1^{(7)} = L_2^{(7)} = 0, L_3^{(7)} = 1$$

(33)

2.4.1 Innumerable Gauss points in triangular element

In 1985, Dunavant provided a method for calculating integrals of polynomial functions on triangular area using Gauss's rules and some laws of mathematics (Dunavant 1985). His rules, which are very efficient in symmetric modes and can be used for finding the integrals of high-degree functions, will be described here.
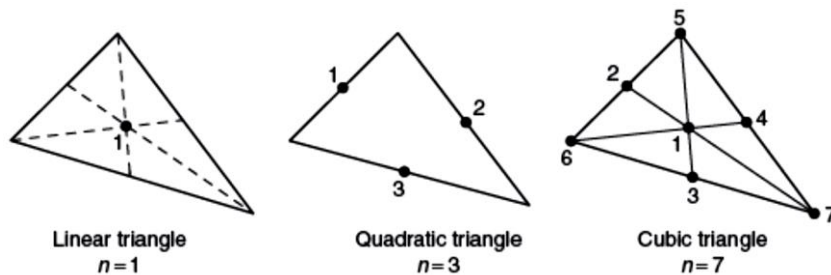

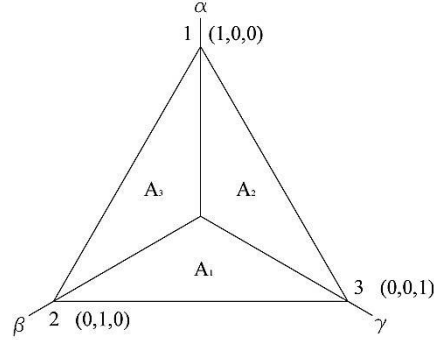Fig. 2 Locations of the integration points

Fig. 3 Barycentric coordinates

Since solving an integral is time-consuming and cumbersome, usually Gauss method is used. This famous method for triangular elements would be in terms of barycentric coordinates which is defined in Fig. 3 (Dunavant 1985).

Integrals of the desired functions on the triangular area using Gauss's law in general form can be expressed as follows

$$\int_A f(\alpha,\beta,\gamma)dA = A\sum_{i=1}^{ng} w_i f(\alpha_i,\beta_i,\gamma_i)$$

(34)

where w_i is the weight associated with the ith Gaussian point of location $(\alpha_i,\beta_i,\gamma_i)$, and ng is the number of sampling points. Accordingly, in order to evaluate the integral, the function shall be evaluated at several sampling points, multiplied by an appropriate weight w_i, and added. By successive application of product rules and using the changes of variables one can reach the following relation (Dunavant 1985)

$$\int_A f(\alpha,\beta,\gamma)dA = \frac{A}{4}\sum_{i=1}^{m} w_i\left(1-u_i\right)\sum_{j=1}^{n} w_i f\left(\alpha_i,\beta_i,\gamma_i\right)$$

(35)

in which, the Gaussian points and weights in the u direction are u_i and w_i, and in the v direction are u_j and w_j respectively.

It is worth mentioning that for an arbitrary complete polynomial of order p, number of terms can be determined using

$$np = \frac{(p+1)(p+2)}{2}$$

(36)

as an example consider $p=2$, knowing that $\alpha + \beta + \gamma - 1 = 0$, then

$$f(\alpha,\beta) = \begin{bmatrix} 1 & \alpha & \beta & \alpha^2 & \alpha\beta & \beta^2 \end{bmatrix}\{a\}$$

(37)

where, $\{a\}$ is polynomial coefficients vector. With the following simple formula, which is for integration of polynomial terms in natural coordinates, the left-hand side of (35) can be obtained

$$\int_A \alpha^i \beta^i dA = 2A \frac{i! \, j!}{(i+j+2)!}$$

(38)

therefore

$$\int_A f(\alpha,\beta) dA = \frac{A}{12}[12,4,4,2,1,2]$$

(39)

and then the right-hand side of (35) is

$$A\sum_{i=1}^{ng} w_i f(\alpha_i,\beta_i) = Aw_1 \begin{bmatrix} 1 & \alpha_1 & \beta_1 & \alpha_1^2 & \alpha_1\beta_1 & \beta_1^2 \end{bmatrix}\{a\}+...$$
$$+Aw_i \begin{bmatrix} 1 & \alpha_i & \beta_i & \alpha_i^2 & \alpha_i\beta_i & \beta_i^2 \end{bmatrix}\{a\}+...$$
$$+Aw_{ng} \begin{bmatrix} 1 & \alpha_{ng} & \beta_{ng} & \alpha_{ng}^2 & \alpha_{ng}\beta_{ng} & \beta_{ng}^2 \end{bmatrix}\{a\}$$

(40)

by equating the right-hand sides of (39) and (40) and reduction of dependent equations, one can write

$$0 = \sum_{i=1}^{ng} w_i - 1$$

(41)

$$0 = \sum_{i=1}^{ng} w_i \gamma_i^2 - \frac{1}{6}$$

(42)

The number of independent equations for different values of p is obtained by

$$m = \frac{(p+3)^2 + \alpha_p}{12}$$

(43)

in which for $p=0$ to 5

$$\alpha_p = +3, -4, -1, 0, -1, -4$$

(44)

Since the reduction in the number of equations by algebraic operations for higher values of p is cumbersome, instead of the natural triangle coordinates, the triangle shown in Fig. 4 is considered, and the polynomials are expressed in polar coordinates (Dunavant 1985).

Thereafter, the moment equations are as follows (Dunavant 1985)

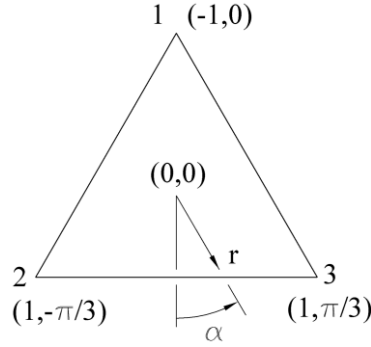$$w_0 + \sum_{i=1}^{n_1} w_i + \sum_{i=n_1+1}^{n_1+n_2} w_i = v_{0,0} = 1$$

(45)

Fig. 4 Triangle polar coordinates

$$\sum_{i=1}^{n_1} w_i r_i^j + \sum_{i=n_1+1}^{n_1+n_2} w_i r_i^j \cos(3k\alpha_i) = v_{j,3k}$$

(46)

where

$$2 \le j \le p, \ 0 \le 3k \le j$$

(47)

and

$$j + 3k = \text{even}$$

(48)

By using symmetry and some mathematical operations the polar moments are as follows (Dunavant 1985)

$$v_{j,3k} = \frac{1}{(j+2)2j\sqrt{3}} \int_{-\frac{\pi}{3}}^{\frac{\pi}{3}} \frac{\cos 3ka}{(\cos a)^{j+2}} \ da$$

(49)

Reference (Dunavant 1985) has classified Gaussian points and weights into three groups. Moreover, values of m, $(j, 3k)$ and $v_{j,3k}$ are tabulated in this reference for up to $m = 44$ corresponding to $p = 20$. It is worth mentioning that the total number of unknowns is

$$n = n_0 + 2n_1 + 3n_2$$

(50)

and the number of Gaussian points is

$$ng = n_0 + 3n_1 + 6n_2$$

(51)

Values of n_1 and n_2 can be determined through (Lyness and Jespersen 1975)

$$n_1 = \left[\left(E(d) - 3n_2 \right) / 2 \right]$$

(52)

and

$$n_2 = \left[\left(E_2(d) + 2 \right) / 3 \right]$$

(53)

in which

$$E(d) = \frac{1}{12} \left((d+3)^2 + \alpha_d \right)$$

(54)

$$E_2(d) = E(d-6) = \frac{1}{12} \left((d-3)^2 + \alpha_d \right)$$

(55)

Moreover, for obtaining the value of n_0, it is required that (Lyness and Jespersen 1975)

$$n_0 + 2n_1 + 3n_2 \geq E(d)$$

(56)

Extracting Gauss Points and Weights

By utilizing relations presented in previous section for a function of degree 12, which is the main topic of this research, a system of nonlinear equations having 19 unknowns including $w_1, w_2, w_3, w_4, w_5, w_6, w_7, w_8, r_1, r_2, r_3, r_4, r_5, r_6, r_7, r_8, \alpha_6, \alpha_7$ and α_8 will be formed

$$w_1 + w_2 + w_3 + w_4 + w_5 + w_6 + w_7 + w_8 = 1$$

$$w_1 r_1^2 + w_2 r_2^2 + w_3 r_3^2 + w_4 r_4^2 + w_5 r_5^2 + w_6 r_6^2 + w_7 r_7^2 + w_8 r_8^2 = \frac{1}{4}$$

$$w_1 r_1^3 + w_2 r_2^3 + w_3 r_3^3 + w_4 r_4^3 + w_5 r_5^3 + w_6 r_6^3 \cos(3\alpha_6) + w_7 r_7^3 \cos(3\alpha_7) + w_8 r_8^3 \cos(3\alpha_8) = -\frac{1}{10}$$

$$w_1 r_1^4 + w_2 r_2^4 + w_3 r_3^4 + w_4 r_4^4 + w_5 r_5^4 + w_6 r_6^4 + w_7 r_7^4 + w_8 r_8^4 = \frac{1}{10}$$

$$w_1 r_1^5 + w_2 r_2^5 + w_3 r_3^5 + w_4 r_4^5 + w_5 r_5^5 + w_6 r_6^5 \cos(3\alpha_6) + w_7 r_7^5 \cos(3\alpha_7) + w_8 r_8^5 \cos(3\alpha_8) = -\frac{2}{35}$$

$$w_1 r_1^6 + w_2 r_2^6 + w_3 r_3^6 + w_4 r_4^6 + w_5 r_5^6 + w_6 r_6^6 + w_7 r_7^6 + w_8 r_8^6 = \frac{29}{560}$$

$$w_1 r_1^6 + w_2 r_2^6 + w_3 r_3^6 + w_4 r_4^6 + w_5 r_5^6 + w_6 r_6^6 \cos(6\alpha_6) + w_7 r_7^6 \cos(6\alpha_7) + w_8 r_8^6 \cos(6\alpha_8) = \frac{1}{28}$$

$$w_1 r_1^7 + w_2 r_2^7 + w_3 r_3^7 + w_4 r_4^7 + w_5 r_5^7 + w_6 r_6^7 \cos(3\alpha_6) + w_7 r_7^7 \cos(3\alpha_7) + w_8 r_8^7 \cos(3\alpha_8) = -\frac{1}{28}$$

$$w_1 r_1^8 + w_2 r_2^8 + w_3 r_3^8 + w_4 r_4^8 + w_5 r_5^8 + w_6 r_6^8 + w_7 r_7^8 + w_8 r_8^8 = \frac{11}{350}$$

$$w_1 r_1^8 + w_2 r_2^8 + w_3 r_3^8 + w_4 r_4^8 + w_5 r_5^8 + w_6 r_6^8 \cos(6\alpha_7) + w_7 r_7^8 \cos(6\alpha_7) + w_8 r_8^8 \cos(6\alpha_8) = \frac{1}{40}$$

$$w_1 r_1^9 + w_2 r_2^9 + w_3 r_3^9 + w_4 r_4^9 + w_5 r_5^9 + w_6 r_6^9 \cos(3\alpha_7) + w_7 r_7^9 \cos(3\alpha_7) + w_8 r_8^9 \cos(3\alpha_8) = -\frac{37}{1540}$$

$$w_1 r_1^9 + w_2 r_2^9 + w_3 r_3^9 + w_4 r_4^9 + w_5 r_5^9 + w_6 r_6^9 \cos(9\alpha_7) + w_7 r_7^9 \cos(9\alpha_7) + w_8 r_8^9 \cos(9\alpha_8) = -\frac{1}{55}$$

$$w_1 r_1^{10} + w_2 r_2^{10} + w_3 r_3^{10} + w_4 r_4^{10} + w_5 r_5^{10} + w_6 r_6^{10} + w_7 r_7^{10} + w_8 r_8^{10} = \frac{13}{616}$$

$$w_1 r_1^{10} + w_2 r_2^{10} + w_3 r_3^{10} + w_4 r_4^{10} + w_5 r_5^{10} + w_6 r_6^{10} \cos(6\alpha_7) + w_7 r_7^{10} \cos(6\alpha_7) + w_8 r_8^{10} \cos(6\alpha_8) = \frac{1}{55}$$

$$w_1 r_1^{11} + w_2 r_2^{11} + w_3 r_3^{11} + w_4 r_4^{11} + w_5 r_5^{11} + w_6 r_6^{11} \cos(3\alpha_6) + w_7 r_7^{11} \cos(3\alpha_7) + w_8 r_8^{11} \cos(3\alpha_8) = -\frac{49}{2860}$$

$$w_1 r_1^{11} + w_2 r_2^{11} + w_3 r_3^{11} + w_4 r_4^{11} + w_5 r_5^{11} + w_6 r_6^{11} \cos(9\alpha_6) + w_7 r_7^{11} \cos(9\alpha_7) + w_8 r_8^{11} \cos(9\alpha_8) = -\frac{2}{143}$$

$$w_1 r_1^{12} + w_2 r_2^{12} + w_3 r_3^{12} + w_4 r_4^{12} + w_5 r_5^{12} + w_6 r_6^{12} + w_7 r_7^{12} + w_8 r_8^{12} = \frac{425}{28028}$$

$$w_1 r_1^{12} + w_2 r_2^{12} + w_3 r_3^{12} + w_4 r_4^{12} + w_5 r_5^{12} + w_6 r_6^{12} \cos(6\alpha_6) + w_7 r_7^{12} \cos(6\alpha_7) + w_8 r_8^{12} \cos(6\alpha_8) = \frac{137}{10010}$$

$$w_1 r_1^{12} + w_2 r_2^{12} + w_3 r_3^{12} + w_4 r_4^{12} + w_5 r_5^{12} + w_6 r_6^{12} \cos(12\alpha_6) + w_7 r_7^{12} \cos(12\alpha_7) + w_8 r_8^{12} \cos(12\alpha_8) = \frac{1}{91}$$

As mentioned earlier, w_i represents Gaussian weights and r_i is the point radial distance from the center of the triangle. Solving the system of equations with a numerical method releases the unknowns as follows

w_1	0.07719319932	r_1	0.4646521693		
w_2	0.1310776336	r_2	0.3191731769		
w_3	0.1885746727	r_3	-0.186368845		
w_4	0.1043883388	r_4	-0.6172715634		
w_5	0.01849878315	r_5	-0.9360479486		
w_6	0.2422293466	r_6	0.4361200406	α_6	0.7230991102
w_7	0.1341406392	r_7	0.5880308643	α_7	0.6566569228
w_8	0.1038973867	r_8	0.7909154485	α_8	0.9479205829

Moreover, obtaining the values of α, β and γ, leads to the location of 33 Gauss points which are tabulated in following table (Dunavant 1985) and can be seen in Fig. 5.

The 33 obtained Gauss points will be employed to calculate time consuming integrals of degree 12, conveniently in short period of time.
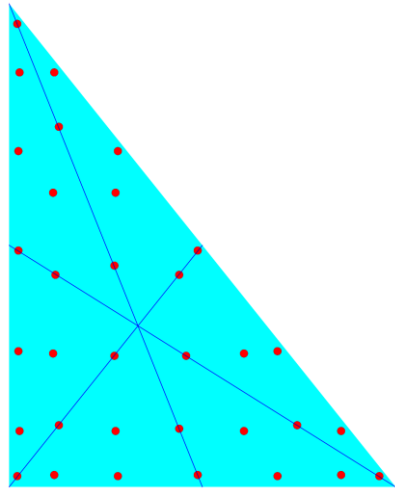
Fig. 5 Location of 33 Gauss points

Table 1 Gauss coordinates for *p*=12

weight	α	β	γ
0.025731066440455	0.023565220452390	0.488217389773805	0.488217389773805
0.043692544538038	0.120551215411080	0.439724392294460	0.439724392294460
0.062858224217885	0.457579229975768	0.271210385012116	0.271210385012116
0.034796112930709	0.744847708916828	0.127576145541586	0.127576145541586
0.006166261051559	0.957365299093580	0.021317350453210	0.021317350453210
0.040371557766381	0.115343494534698	0.275713269685514	0.608943235779788
0.022356773202303	0.022838332222257	0.281325580989940	0.695836086787803
0.017316231108659	0.025734050548330	0.116251915907597	0.858014033544073

3. Rectangular reservoir dynamic analysis

Herein, dynamic analysis of free vibration of the fluid within the rectangular reservoir is performed. The analysis is conducted by using the exact and finite element methods, and frequencies of the reservoir are obtained by different ratios of length to depth.

3.1 Closed-form solution

Using Fourier transformation, Helmholtz equation (Eq. (17)) can be transferred to frequency domain

$$w = \pi c \sqrt{\left(\frac{m}{a}\right)^2 + \left(\frac{2n-1}{2b}\right)^2}$$

(57)

by which natural frequencies of the free vibration of the rectangular reservoir could be obtained. In Eq. (57), c is the velocity of pressure waves in water and b is the depth of the reservoir assumed to be equal to 1440 meters per second, and 200 meters respectively. By solving the above equation 10 first natural frequencies of the reservoir for different ratios of length to depth (a/b) are calculated and tabulated in Table 2.

3.2 Fluid Analysis by means of FEM

In this part, the analysis of the problem by using the finite element method with the aid of a computer program (Mathematica) is discussed. Different length to depth ratios of reservoir is considered in order to observe the impacts of reservoir length changes on the natural frequencies of the fluid. In Fig. 6, the finite element model of a typical rectangular reservoir model with the ratio of the length to depth of three is displayed in which eight-node quadratic elements are used.

Following table and chart demonstrate the results of analysis of reservoirs with different length to depth ratios.

3.3 Comparison between closed form and analytical solutions

Comparing the results of dynamic analysis of the reservoir using finite element method expressed in previous section and responses obtained by closed form solution, can validate the accuracy of finite element method responses and the related developed computer program. Table 4 shows obtained natural frequencies and errors due to numerical analysis:

Table 2 natural frequencies of closed form solution

Mode No.	Length/Depth=1	Length/Depth=2	Length/Depth=3	Length/Depth=4
1	1.8000	1.8000	1.8000	1.8000
2	4.0249	2.5456	2.1633	2.0125
3	5.4000	4.0249	3.0000	2.5456
4	6.4900	5.4000	4.0249	3.2450
5	7.4216	5.6921	5.1264	4.0249
6	9.0000	5.6921	5.4000	4.8466
7	9.0000	6.4900	5.5317	5.4000
8	9.6933	7.4216	5.9093	5.4745
9	10.9490	7.6368	6.2642	5.6921
10	11.5256	9.0000	6.4900	5.6921

As can be seen in Table 4, the responses obtained from the free vibration analysis of rectangular reservoir with aid of finite elements are in a very good agreement with the results of exact solution. The most important reason can be this fact that quadratic elements are used rather than tow-linear four-node elements. Moreover, greater natural frequencies obtained from finite element method compared to the exact solution was predictable, since the application of approximate interpolation functions make model stiffer.
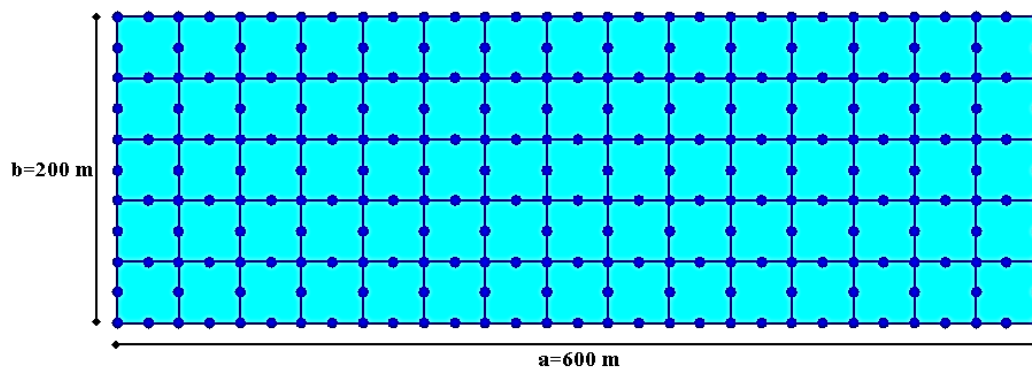

Fig. 6 Typical reservoir model

Table 4 Comparison between natural frequencies of closed form and FEM results

| Mode No.	Length/Depth=1			Length/Depth=2			Length/Depth=3			Length/Depth=4		
	Closed form	FE analysis	Error (%)	Closed form	FE analysis	Error (%)	Closed form	FE analysis	Error (%)	Closed form	FE analysis	Error (%)
1	1.8000	1.800	0.001	1.8000	1.800	0.001	1.8000	1.800	0.001	1.8000	1.800	0.001
2	4.0249	4.025	0.009	2.5456	2.546	0.004	2.1633	2.163	0.002	2.0125	2.013	0.008
3	5.4000	5.403	0.052	4.0249	4.025	0.009	3.0000	3.000	0.002	2.5456	2.546	0.000
4	6.4900	6.493	0.041	5.4000	5.403	0.052	4.0249	4.025	0.009	3.2450	3.245	0.002
5	7.4216	7.433	0.151	5.6921	5.695	0.047	5.1264	5.128	0.029	4.0249	4.025	0.009
6	9.0000	9.012	0.135	5.6921	5.695	0.047	5.4000	5.403	0.052	4.8466	4.848	0.023
7	9.0000	9.034	0.375	6.4900	6.493	0.041	5.5317	5.534	0.050	5.4000	5.403	0.052
8	9.6933	9.725	0.331	7.4216	7.433	0.151	5.9093	5.912	0.045	5.4745	5.477	0.051
9	10.9490	11.028	0.722	7.6368	7.641	0.057	6.2642	6.269	0.072	5.6921	5.695	0.047
10	11.5256	11.568	0.371	9.0000	9.012	0.135	6.4900	6.493	0.041	5.6921	5.695	0.047
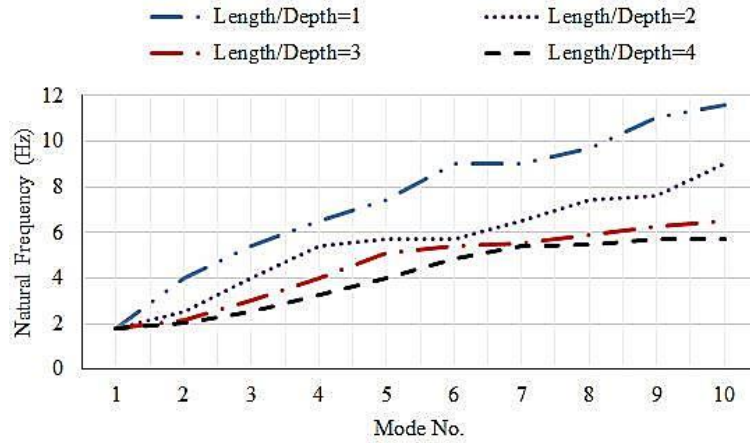
Fig. 7 Changes of natural frequencies for different *L/D* ratios

4. Free vibration analysis of ideal triangular dam

In this section, free vibration analysis of ideal right triangular dam is carried out. It is noteworthy that human do not yet have an exact solution to this problem. In the following subdivision, the analysis of dam by eight and twenty-one node elements would be explained.

4.1 Modeling by 8-Node element

The ideal dam modelled by eight-node triangular elements which analysis would be performed by a program written in the mathematical software Mathematica, is shown in Fig. 8. Dam height and foundation length are 200 and 160 meters, respectively. Furthermore, density, modulus of elasticity and Poisson's ratio of the used concrete are equal to 2528 kg/m3, 27.5 Gpa and 0.2, respectively.
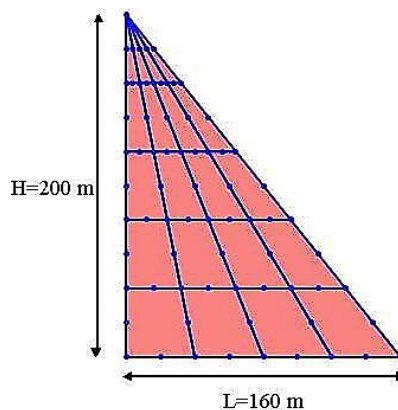

Fig. 8 Dam modelled by eight-node triangular elements

Table 5 Natural frequencies of dam (modeled with 20 elements)

Mode No.	Natural Frequency (Hz)
1	2.28766
2	5.19004
3	6.03763
4	8.9302
5	13.17190
6	13.3479
7	16.0823
8	17.1728
9	18.5568
10	20.3533

As it can be seen in Fig. 8, dam consists of twenty elements and seventy one nodes. Each node has two degrees of freedom with horizontal and vertical displacements. It should be noted that, the base of the triangle is connected to the ground by fixed joints and bottom nodes do not have any degrees of freedom. Hence, total degrees of freedom of the dam is one hundred and twenty four, which is exactly equal to the dimensions of mass and stiffness matrices.

The developed program firstly, calculates mass and stiffness matrices for all elements. Afterwards, they would be assembled and eigenvalue problem would be created (Eq. (14)). Solving the eigenvalue problem releases natural frequencies of the dam. Table 5 shows the results of free vibration analysis of the dam.

Furthermore, ten first mode shapes of the dam are displayed in the Fig. 9.

4.2 Introducing of 21-node element

Herein the aforesaid dam would be analyzed with the help of only one twenty-one-node triangular element instead of eight-node elements. The appropriate interpolation functions could be obtained by utilizing full fifth-degree polynomial functions. For this purpose, firstly, mass and stiffness matrices are calculated and then the eigenvalues and dam natural frequencies are extracted. It should be mentioned that, the analysis would be carried out in two ways; once the mass and stiffness matrices are computed with the precise integrating which is time-consuming and cumbersome, and the other time, Gauss integration will be used. It is noteworthy that the method for obtaining the Gauss points is explained in section 2.4. Moreover, it is worth noting that boundary conditions remain the same for this element. Fig. 10 shows the ideal triangular dam which is modelled by one twenty-one-node element.

Free vibration analysis results conducted with only one twenty-one-node element can be seen in table 6. Moreover, Fig. 11 compares the results obtained by using two different elements.
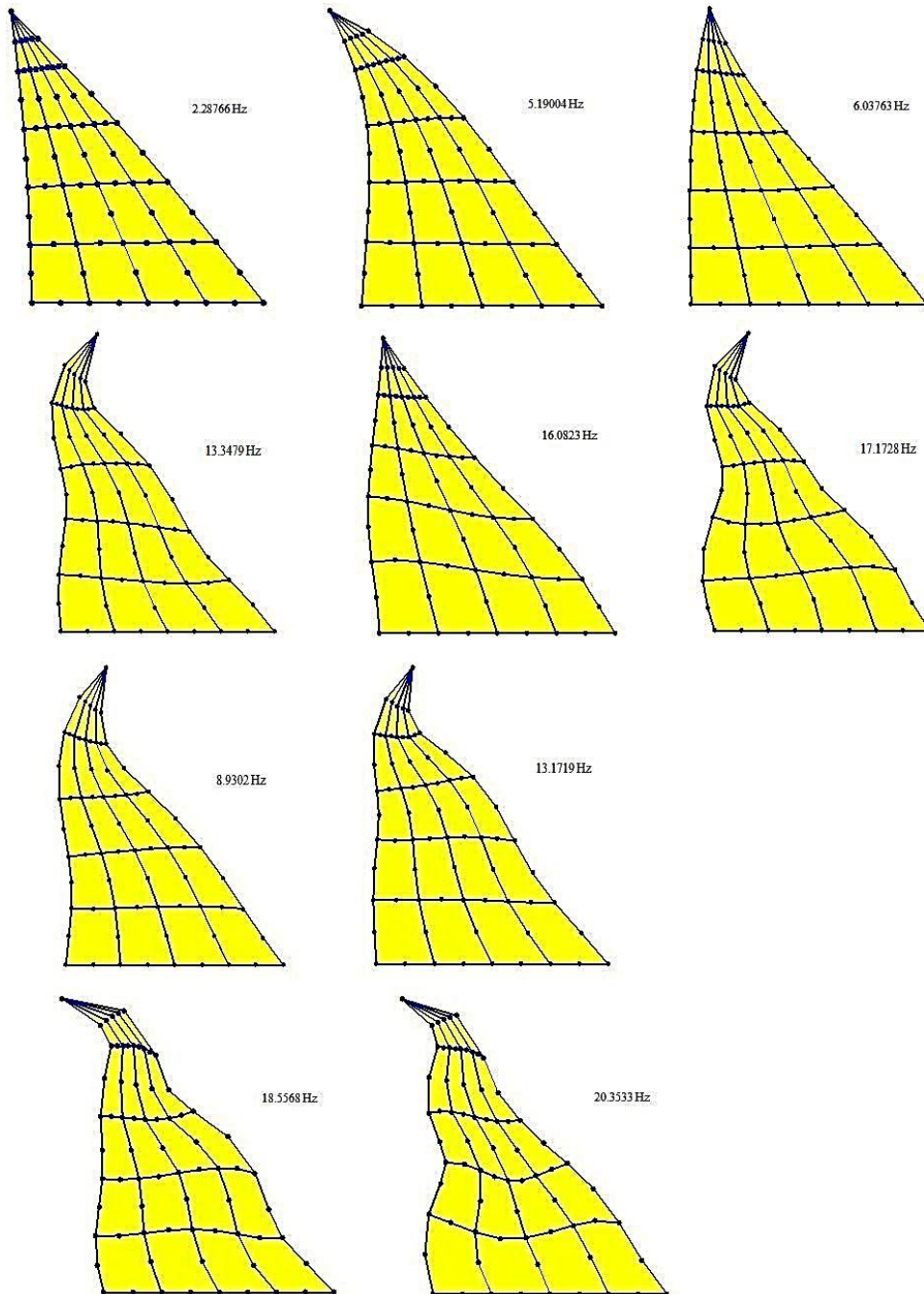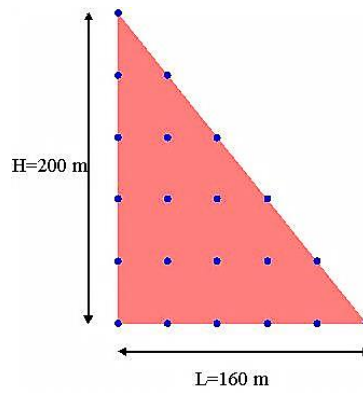
Fig. 9 Mode shapes of triangular Dam (20 elements)

Fig. 10 Dam modeled with one element

Table 6 Natural frequencies of dam (modeled with one element)

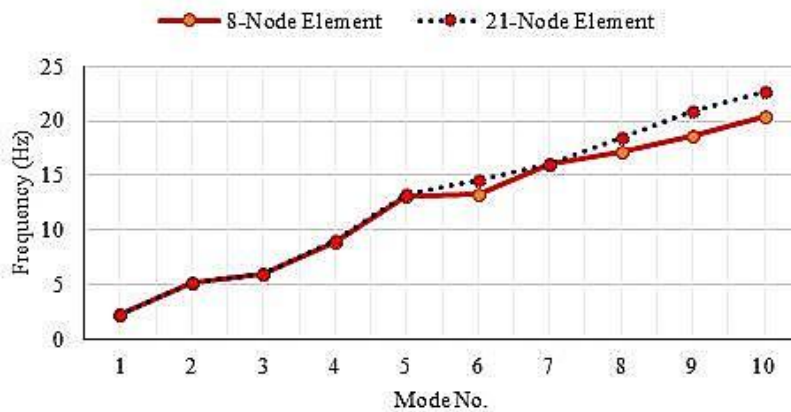| Mode No.	Natural Frequency (Hz)
1	2.28766
2	5.17996
3	6.03582
4	9.00004
5	13.2516
6	14.6035
7	16.1159
8	18.4042
9	20.8832
10	22.6872

Fig. 11 Comparison between frequencies of dam models

Smaller frequencies in the first three modes of the 21-node element diagram compared to 8-node element diagram, indicates that the values obtained from the dam analysis with twenty-one-node element are more accurate in the lower modes than values obtained from the dam analysis with eight-node elements.
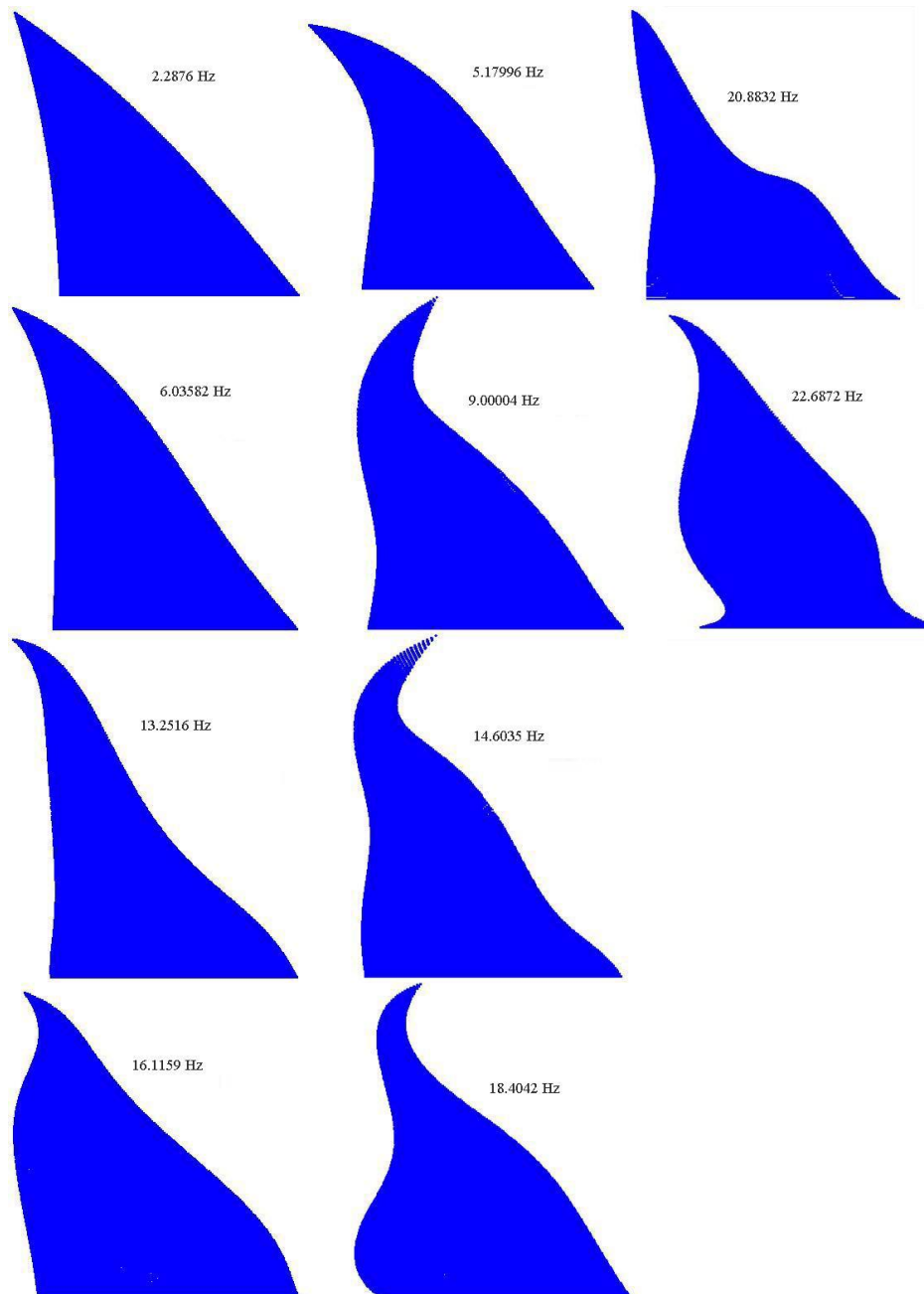

Fig. 12 Mode shapes of triangular Dam (one element)

In order to draw mode shapes, a special technique is used. For eight-node elements model, firstly, node displacements were calculated and then, by connecting the deformed nodal points to each other, the mode shapes were extracted. Herein, for drawing dam deformation a large number of lines with same intercepts are considered. Line intercepts assumed to be equal to 200 meters in order to pass through the dam crest. Consequently, one can obtain the equation of the lines and find the corresponding points on each line to identify the new position of each point and plot the relevant mode shape which can be seen in Fig. 12.

5. Interaction analysis of dam-reservoir by 21-node element

The fifth section which is the most important part of this research from innovative perspective, is devoted to the interaction analysis of the gravity dam-reservoir system, by the twenty-one-node element and the aid of thirty-three Gauss points.

5.1 Dam modeling by 21-node element with numerous Gauss points

Previously, in part 4.2, the twenty-one-node triangular element and the model of gravity dam constructed by only one element was introduced. Therein, the necessary integrations for obtaining the mass and stiffness matrices were carried out in an accurate but time consuming way (about an hour and a half for each matrix), using Mathematica program. But here, due to the introduced efficient and effective Gauss integration method with numerous Gauss points in section 2.4.1, the calculation will be conducted again with the same precision in a much faster process (about one second for each matrix). Afterwards, dam model with Gauss points is displayed and it is avoided publishing results for brevity. It is obvious that with respect to selection of a large number of Gauss points, the results of numerical integration will be exactly the same as the results of the accurate integration. Fig. 13 shows the ideal model of the triangular dam, made up of only one twenty-one node element. Note that the larger and the smaller points are element nodes and points of Gauss, respectively.
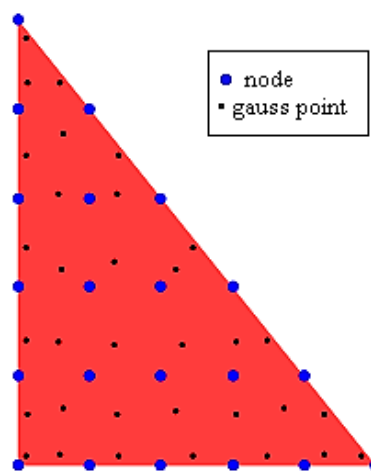

Fig. 13 Dam model with 21 node-33 gauss point element

5.2 Reservoir modeling by 21-node element with numerous Gauss points

After introducing the ideal model of the triangular dam made up of only one twenty-one node element, herein, the fluid in the rectangular reservoir will be modelled for four different length to depth ratios utilizing two, four, six, and eight 21-node-element, again with 33 Gauss points. After the free vibration analysis, the natural frequencies of the fluid, itself, will be extracted. It is noteworthy that the natural frequencies were obtained for the mentioned states in accurate (non-numerical) and finite element (numerical) methods previously in section 3, but with help of eight-node elements. The reservoir model and the natural frequencies obtained from the analysis are presented in the following table and figure.

Table 7 Natural frequencies of dam (modeled with 21 node-33 gauss point element)

| Mode No.	Length/Depth=1	Length/Depth=2	Length/Depth=3	Length/Depth=4
1	1.80000	1.80000	1.80000	1.80000
2	4.02504	2.54558	2.16333	2.01246
3	5.40061	4.02504	3.00001	2.54558
4	6.50268	5.40061	4.02504	3.24501
5	7.44700	5.69533	5.12738	4.02504
6	9.06628	5.69746	5.40061	4.84725
7	9.18883	6.50268	5.53302	5.40061
8	9.95085	7.44700	5.91375	5.47546
9	11.19290	7.66395	6.26954	5.69533
10	12.07020	9.06628	6.50268	5.69746
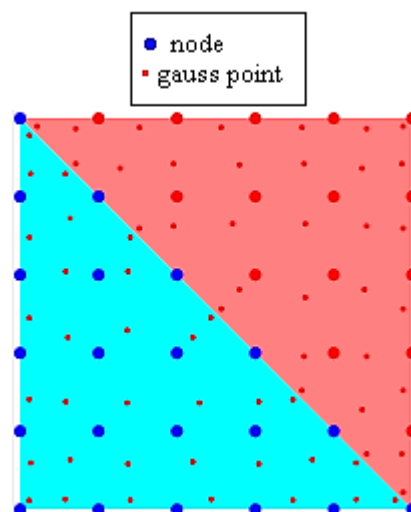
Fig. 14 Reservoir model with 21 node-33 gauss point element (L/D=1)

5.3 Results for dam-reservoir interaction

Up to here, dam and the reservoir were analyzed independently. In this section, the model of interacted dam-reservoir will be constructed and its free vibration will be analyzed utilizing twenty-one-node elements. Outcome of the analysis is the coupled natural frequencies of the system which are smaller than decoupled natural frequencies of components in each vibration mode. Similar to previous section, the coupled dam-reservoir model and natural frequencies of free vibration are provided in Table 7 and Fig.15.

Moreover, the results from the analysis of dam itself, the fluid in the rectangular reservoir with a length of two hundred meters, and gravity dam- rectangular reservoir with the same length-system are compared in table 9 to denote the difference between the dynamic behaviors of coupled system with each of the single components.

Table 8 Natural frequencies of reservoir (modeled with 21 node-33 gauss point elements)

| Mode No.	Length/Depth=1	Length/Depth=2	Length/Depth=3	Length/Depth=4
1	1.54206	1.59801	1.61228	1.61618
2	2.17812	2.00697	1.91681	1.86946
3	3.91873	2.67144	2.32627	2.17080
4	4.96998	3.96430	3.04035	2.61666
5	5.45902	4.82698	3.98242	3.26152
6	5.93840	5.42215	4.73056	3.99217
7	6.60330	5.69443	5.26616	4.64049
8	7.49872	5.81974	5.41708	5.03833
9	8.55207	5.99300	5.56806	5.40981
10	9.08954	6.56996	5.87140	5.49861
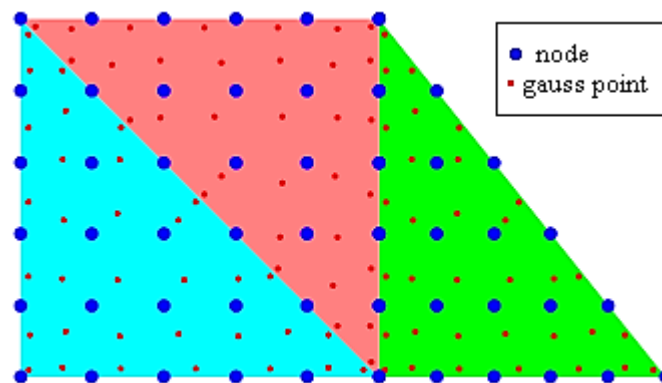
Fig. 15 Reservoir model with 21 node-33 gauss point element (L/D=1)

Table 9 Comparison between natural frequencies of dam, reservoir and the coupled system

Mode No.	Sole dam	Sole Fluid	Coupled System
1	2.28766	1.80000	1.54206
2	5.17996	4.02504	2.17812
3	6.03582	5.40061	3.91873
4	9.00004	6.50268	4.96998
5	13.2516	7.44700	5.45902
6	14.6035	9.06628	5.93840
7	16.1159	9.18883	6.60330
8	18.4042	9.95085	7.49872
9	20.8832	11.1929	8.55207
10	22.6872	12.0702	9.08954

6. Conclusions

The main objective of this research involved the free vibration dynamic analysis of gravity dam-rectangular reservoir system. This analysis was performed in the frequency domain and the final results included frequency and shape modes of the system. It is worth noting that all the analysis was carried out using finite element method and the problem domain was modeled by eight and twenty-one-node elements.

The research was carried out in this pattern that sections one and two provided the necessary theoretical foundations in which the method for extracting the key points and weights corresponding to thirty-three Gauss points for integration of polynomial of degree twelve proportional to triangular area was expressed. Section three was devoted to dynamic analysis of free vibration of the fluid within the rectangular reservoir, wherein the exact solution of reservoir free vibration was described firstly, then finite element method using 8-node elements was applied and finally a comparison was made between results which were natural frequencies. Section four was dedicated to free vibration analysis of ideal triangular dam utilizing eight and twenty-one-node elements. The integrations for twenty-one-node element were performed using accurate procedure. Eventually, section five illustrated the dam-reservoir coupled system analysis using twenty-one-node elements and utilizing thirty-three Gauss points, and the obtained results were compared in tables. In this section different length to depth ratios of the reservoir were considered.

Some qualitative consequences achieved from the quantitative results of this research are as follows:

1. With regard to the third section, one can realize that the finite element method is a very efficient and powerful method for free vibration analysis of compressible inviscid fluids.
2. Interestingly, the results of the analysis of the right triangle with only one twenty-one-node element in the first three modes of vibration, which are the most important modes, were more accurate than the results from the model made by twenty quadratic eight-node-elements which has seventy-one nodes totally (having 50 nodes and 100

degrees of freedom more than five-degree-element). It is noteworthy that due to this fact that the possibility of obtaining an exact solution and closed formulation for the free vibration analysis of a right triangle has not been provided yet, for obtaining much more pleasant estimation, the accuracy of interpolation functions were increased by enhancing their degree which leads to the creation of a new twenty-one-node-triangular element that the base of its shape functions was formed with a complete polynomial of degree 5.

3. Time needed for the analysis of coupled dam-reservoir system was reduced thousands times by taking advantages of Gauss integration method with 33 points and utilizing twenty-one-node elements for both structure and fluid.

Refrences

Attarnejad, R. and Kalateh, F. (2012), "Numerical simulation of acoustic cavitation in the reservoir and effects on dynamic response of concrete dams", *Int. J. Civil Eng*., **10**, 72-86.

Bouaanani, N. and Lu, F.Y. (2009), "Assessment of potential-based fluid finite elements for seismic analysis of dam–reservoir systems", *Comput. Struct*., **87**, 206-224.

Burman, A., Nayak, P., Agrawal, P. and Maity, D. (2012), "Coupled gravity dam–foundation analysis using a simplified direct method of soil–structure interaction", *Soil Dynam. Earthq. Eng*., **34**(1), 62-68.

Calayir, Y. and Karaton, M. (2005), "A continuum damage concrete model for earthquake analysis of concrete gravity dam–reservoir systems", *Soil Dynam. Earthq. Eng*., **25**(11), 857-869.

Dunavant, D.A. (1985), "High degree efficient symmetrical Gaussian quadrature rules for the triangle", *Int. J. Numer. Meth. Eng*., **21**(6), 129-148.

Fenves, G. and Chopra, A.K. (1984), "Earthquake analysis of concrete gravity dams including reservoir bottom absorption and dam-water-foundation rock interaction", *Earthq. Eng. Struct. D*., **12**(5), 663-680.

Ghaemian, M. and Ghobarah, A. (1999), "Nonlinear seismic response of concrete gravity dams with dam–reservoir interaction", *Eng. Struct*., **21**(4), 306-315.

Hall, J.F. and Chopra, A.K. (1982), "Hydrodynamic effects in the dynamic response of concrete gravity dams", *Earthq. Eng. Struct. D*., **10**(2), 333-345.

Hariri-Ardebili, M.A., Mirzabozorg, H. and Ghasemi, A. (2013), "Strain-based seismic failure evaluation of coupled dam-reservoir-foundation system", *Coupled Syst. Mech*., **2**(1), 85-110.

Karaca, MA. And Küçükarslan, S. (2012), "Analysis of dam-reservoir interaction by using homotopy analysis method", *KSCE J. Civil Eng*., **16**(1), 103-106.

Keivani, A., Shooshtari, A. and Aftabi Sani, A. (2014), "Forced vibration analysis of a dam-reservoir interaction problem in frequency domain", *Coupled Syst. Mech*., **3**(4), 385-403.

Leger, P. and Bhattacharjee, S.S. (1992), "Reduced frequency-independent models for seismic analysis of concrete gravity dams", *Comput. Struct*., **44**(6), 1381-1387.

Lyness, J.N. and Jespersen, D. (1975), "Moderate degree symmetric quadrature rules for the triangle", *J. Inst. Math. Appl*., **15**(1), 19-32.

Miquel, B. and Bouaanani, N. (2010), "Simplified evaluation of the vibration period and seismic response of gravity dam-water systems", *Eng. Struct*., **32**(8), 2488-2502.

Miquel, B. and Bouaanani, N. (2011), "Practical dynamic analysis of structures laterally vibrating in contact with water", *Comput. Struct*., **89**(23-24), 2195-2210.

Mirzayee, M., Khaji, N. and Ahmadi, M.T. (2011), "A hybrid distinct element–boundary element approach for seismic analysis of cracked concrete gravity dam–reservoir systems", *Soil Dynam. Earthq. Eng*., **31**(10), 1347-1356.

Mridha, S. and Maity, D. (2014), "Experimental investigation on nonlinear dynamic response of concrete gravity dam-reservoir system", *Eng. Struct*., **80**, 289-297.

Rao, S.S. (2011), "The Finite Element Method in Engineering", Burlington, MA 01803, USA.

Samii, A. and Lotfi, V. (2007), "Comparison of coupled and decoupled modal approaches in seismic analysis of concrete gravity dams in time domain", *Finite Elem. Anal. Des.*, **43**, 1003-1012.

Valliappan, S. amd Zhao, C. (1992), "Dynamic response of concrete gravity dams including dam-water-foundation interaction", *Int. J. Numer. Anal. Meth. Geomech.*, **16**(2), 79-99.

Yazdchi, M., Khalili, N. and Valliappan, S. (1999), "Non-linear seismic behaviour of concrete gravity dams using coupled finite element-boundary element technique", *Int. J. Numer. Meth. Eng.*, **44**(1), 101-130.

Zhao, C., Xu, T.P. and Valliappan, S. (1995), "Seismic response of concrete gravity dams including water-dam-sediment-foundation interaction", *Comput. Struct.*, **54**(4), 705–715.